Oil Shale, 2014, Vol. 31, No. 3, pp. 250–265
doi: 10.3176/oil.2014.3.05
ISSN 0208-189X

PYROLYSIS KINETICS OF NORTH-KOREAN OIL SHALE

WEI WANG[(a)], SHU-YUAN LI[(a)*], LIN-YUE LI[(a)], YUE MA[(a)], CHANG-TAO YUE[(a)], JI-LAI HE[(b)]

[(a)] State Key Laboratory of Heavy Oil Processing, China University of Petroleum, Beijing 102249, China
[(b)] Shandong Energy Longkou Mining Group Co., Ltd, Longkou 265700, China

Abstract. *In this paper, the kinetics of pyrolysis of North-Korean oil shale was investigated. Fischer Assay analysis showed that the oil yield of oil shale sample was 12.14 wt%. Thermogravimetry was applied to the analysis of pyrolysis of oil shale at the heating rates of 5, 10, 15, 20 and 25 °C/min. The kinetic parameters (apparent activation energy E and frequency factor A) were determined by the Friedman procedure, maximum pyrolysis rate method and parallel reactions model, respectively. Based on the Friedman procedure the values of apparent activation energy E were found to range from 209 kJ/mol to 359 kJ/mol and frequency factor A from 6.32 × 10^{12} to 1.99 × 10^{20}·min^{-1}. It was shown by the maximum pyrolysis rate method that E and A were respectively 191.52 kJ/mol and 1.51 × 10^{13}·min^{-1}. As determined by the parallel reactions model, the values of apparent activation energy were mainly between 130 kJ/mol and 240 kJ/mol. The plot of ln A vs E for oil shale pyrolysis was a straight line.*

Keywords: *oil shale, pyrolysis kinetics, apparent activation energy, frequency factor.*

1. Introduction

Oil shale, as a source of chemical feedstocks, has attracted renewed attention due to the uncertainty in the long term about the availability of crude oil supplies, and the world energy crisis [1–3]. Many countries are paying more and more attention to utilization of oil shale to produce energy products. Actually, during the last twenty years, a number of innovative processes have been developed, such as fluidized-bed pyrolysis and hydroretorting, to obtain considerably higher oil yields than by classic retorting procedures [4]. Oil shale is a sedimentary rock containing soluble bitumen and insoluble

* Corresponding author: e-mail *syli@cup.edu.cn*

kerogen. Oil, water, gas and semi-coke are produced through oil shale pyrolysis [5].

Thermogravimetric analysis (TGA) is a widely used method for determination of kinetic parameters of complex reactions. Weight loss information can be used to construct kinetic models of the decomposition process. The method is effective in developing sophisticated models.

Li and Yue [6] studied the kinetics of pyrolysis of different Chinese oil shale samples at a heating rate of 5 °C/min. A special kinetic model involving 11 parallel first-order reactions was developed to obtain a distribution function of apparent activation energy and an equation for the apparent activation energy-frequency factor relationship. This method is used to describe the oil shale pyrolysis in detail. Dogan and Uysal [7] and Torrente and Galan [8] investigated the kinetics of pyrolysis of Turkish oil shale and Spanish oil shale, using isothermal and non-isothermal TGA separately. The kinetic models included regression function, integral method, differential method, Friedman procedure, and maximum rate method. Tiwari and Teo [9] used the advanced isoconversion method to compute the apparent activation energy of the decomposition process. The calculated values were in the range of 92–226 kJ/mol with respect to conversion. Williams and Ahmad [10] investigated the pyrolysis of Pakistani oil shale at varying heating rates. It was found that the temperature of reaction increased with increasing heating rate. The kinetics of thermal decomposition of Tafraya (Morocco) oil shale and kerogen was studied by Aboulkas and El Harfi [11]. The apparent activation energy of materials degradation was determined by Kwassinger-Akahira-Sunose, Friedman, Flynn-Wall-Ozawa and Coats-Redfern methods. Abu-Qudais et al. [12] investigated the kinetics of pyrolysis of Attarat oil shale of Jordan, using a thermogravimetric analyzer. The TGA data were analyzed through the integral method to determine kinetic parameters. In the first stage, the average apparent activation energy was between 13.5 kJ/mol and 16.5 kJ/mol, which confirmed that only physical changes and/or breaking of weak chemical bonds took place. In the second stage, the reactions had much higher values of apparent activation energy, namely in the range of 79.2–91.7 kJ/mol.

A differential thermal analyzer was used for experiments on North-Korean oil shale pyrolysis at the heating rates of 5, 10, 15, 20 and 25 °C/min. The kinetic parameters (apparent activation energy E and frequency factor A) were determined using the Friedman procedure, maximum pyrolysis rate method and parallel reactions model, respectively.

2. Experimental

2.1. Sample

The oil shale sample for investigations was taken from the Anzhou basin, North Korea. Oil shale was deposited during the Jurassic period of the Mesozoic era (ca. 165 Ma) [13]. In the experiments, the sample was crushed

and sieved to eliminate effects of heat transfer and mass transfer of oil shale particles on kinetic parameters. The fraction with a size of less than 200 mesh was taken as the experimental sample. The Fisher Assay was carried out according to ASTM standards (ASTM D3904-90). The proximate and ultimate analyses were performed using an HTGF-3000 analyzer (Thailand), and LECO CHN-2000 and LECO S-144DR analyzers (USA), respectively. The basic properties and results of Fisher Assay and proximate analyses of North-Korean oil shale are presented in Table 1.

Table 1. Fisher Assay and proximate analysis of North-Korean oil shale (air received basis, ar%)

Sample	Fisher Assay, wt%				Proximate analysis, wt%			
	Oil	Water	Semi-coke	Gas	Moisture	Volatile	Ash	Fixed carbon
North-Korean oil shale	12.14	7.74	75.87	4.25	4.27	25.81	52.98	16.94
	C	H	O	N	S	Kerogen type		Vitrinite reflectance
	30.56	3.25	10.19	0.90	5.59	II		0.52

2.2. Apparatus and procedures

A NETZSCH STA409PC TGA instrument (sensitivity 10 ug, balance capacity 20 g; Germany) was employed to investigate the kinetics of pyrolysis of North-Korean oil shale at the heating rates of 5, 10, 15, 20 and 25 °C /min from ambient temperature to 600 °C. The experiments were performed twice to ensure repeatability. The lower rate of heating (5 °C/min) was used to minimize systematic errors in temperature measurement due to thermal lag during pyrolysis.

The experimental conditions were as follows:

- carrier gas: nitrogen with a purity of 99.99%
- flow rate of carrier gas: 60 ml·min^{-1}
- final pyrolysis temperature: 600 °C
- weight of the sample: 10–20 mg
- quartz crucible.

2.3. Mathematical model

It is assumed that oil shale pyrolysis is a first-order reaction, so the kinetic equation of oil shale pyrolysis can be described by the following equation:

$$\frac{dx}{dt} = A\exp\left(-\frac{E}{RT}\right)(1-x). \tag{1}$$

A 3-spline interpolation equation can be used to calculate the rate of pyrolysis of oil shale:

$$\frac{dx}{dT}(T)=\frac{6}{h_j^2}\left[\frac{1}{h_j}(T_{j+1}-T)^2-(T_{j+1}-T)\right]x_j+\frac{6}{h_j^2}\left[(T-T_j)-\frac{1}{h_j}(T-T_j)^2\right]x_{j+1}$$
$$+\frac{1}{h_j}\left[\frac{3}{h_j}(T_{j+1}-T)^2-2(T_{j+1}-T)\right]m_j-\frac{1}{h_j}\left[2(T-T_j)-\frac{3}{h_j}(T-T_j)^2\right]m_{j+1} \quad (2)$$

When solving Equation (2), the boundary conditions are as follows:

$$\frac{d^2x}{dT^2}\Big|_{x\to 0}=\frac{d^2x}{dT^2}\Big|_{x\to 1}=0\,. \quad (3)$$

2.3.1. Friedman procedure

Taking the logarithm of Equation (1) will give the following equations:

$$\ln\frac{dx}{dt}=\ln\left[A(1-x)\right]-\frac{E}{RT}\,. \quad (4)$$

$$\frac{dx}{dt}=\frac{dx}{dT}\times\beta\,. \quad (5)$$

The values of specific temperature (T) and the instantaneous rate of reaction (dx/dT) of oil shale are various when with different heating rates the same stage of conversion is reached. There are five different x-T curves corresponding to five different heating rate values. Set a series of different values of the fractional conversion x (*x1, x2, x3*, …) as constants. According to Equation (4), the linear regression of ln (dx/dt) vs $1/T$ will determine the apparent activation energy E and frequency factor A for each x. The values of E and A corresponding to different x can be determined from x-E and x-A curves.

2.3.2. Maximum rate method

According to mathematical principles, the maximum rate of oil shale pyrolysis is found by the following equation:

$$\frac{d^2x}{dT^2}=\frac{A}{\beta}\frac{E}{RT^2}(1-x)\mathrm{e}^{-E/RT}-\left(\frac{A}{\beta}\mathrm{e}^{-E/RT}\right)^2(1-x)\,. \quad (6)$$

When the reaction rate reaches maximum, then:

$$\frac{d^2x}{dT^2}=0. \quad (7)$$

When T is labeled as T_m, Equation (6) becomes:

$$\frac{\beta}{T_m^2} = \frac{AR}{E} \mathrm{e}^{-E/RT_m} . \tag{8}$$

Taking the logarithm of both sides of Equation (8) will give:

$$\ln \frac{\beta}{T_m^2} = \ln \frac{AR}{E} - \frac{E}{RT_m} . \tag{9}$$

For the same sample, T_m with different heating rates is different. The linear regression of ln (β/T_m^2) vs $1/T_m$ will give the apparent activation energy E and apparent frequency factor A.

2.3.3. Parallel reactions model

In order to study the complicated pyrolysis process of oil shale more precisely, it is assumed that N parallel first-order reactions take place in the pyrolysis process of oil shale with different values of apparent activation energy E_j and apparent frequency factor A_j simultaneously. According to Equation (1), the rate equation for each parallel reaction can be written as follows:

$$\frac{dx_j(T)}{dT} = \frac{A_j}{\beta} \exp\left(-\frac{E_j}{RT}\right)[x_\infty(j) - x_j] . \tag{10}$$

According to the definition and material balance, $x_j(T)$ and $x_\infty(j)$ should be consistent with the following conditions:

$$\begin{aligned} &\sum_{j=1}^{N} x_\infty(j) = 1 \\ &\sum_{j=1}^{N} x_j(T) = x(T) \end{aligned} . \tag{11}$$

Taking the integration of Equation (10) will yield:

$$x(T) = \sum_{j=1}^{N} x_\infty(j) \times \left\{ 1 - \exp\left[-\int_{T_0}^{T} \exp\left(-\frac{E_j}{RT} + \ln A_j - \ln \beta\right) dT \right] \right\} . \tag{12}$$

In Equation (12), experimental data $x(T)$ and T are obtained from weight loss curves. During the calculation, different values of E_j are given in advance. The unknown parameters A_j and $x_\infty(j)$ (j = 1, 2, ..., N) can be determined by the least squares regression. The relative error F can be obtained by Equation (13) to examine regressed conversions between experimental and calculated values:

$$F = \left[\sum_{i=1}^{M} \frac{1}{M} \left(\frac{x_{\text{experimental}} - x_{\text{calculated}}}{x_{\text{experimental}}} \right) \right]. \tag{13}$$

3. Results and discussion

Figure 1 depicts the TG and DTG curves of North-Korean oil shale as a function of temperature at 15 °C/min. The remarkable features of the TG curve are the following: (1) The weight loss curve declines from 100% to 97% below 200 °C due to the evaporation of moisture. The change is just consistent with the high water content (Table 1). (2) The weight loss curve falls sharply from 200 °C to 600 °C due to the release of volatile hydrocarbons, which is the main stage of pyrolysis of the bitumen and kerogen present in oil shale.

Figure 2 shows that the curves of North-Korean oil shale pyrolysis ranging from 200 °C to 600 °C at different heating rates are almost similar and exhibit the same trend. The conversion rate increases slowly at temperatures up to 400 °C, then rises abruptly and grows moderately above 500 °C. When at different heating rates the same stage of conversion is reached, the lower the heating rate, the higher the temperature. Unlike slow heating, rapid heating may reduce the time needed to attain a certain degree of conversion.

Worth of attention is also the fact that the heating rate has almost no effect on the organic matter decomposition under the same operating conditions. In other words, total conversion values in pyrolysis were almost constant at all heating rate values [14].

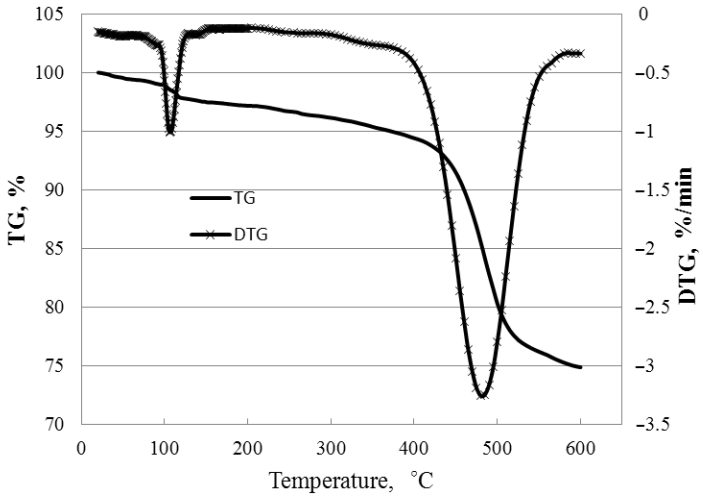

Fig. 1. TG/DTG curves of North-Korean oil shale at a heating rate of 15 °C/min.

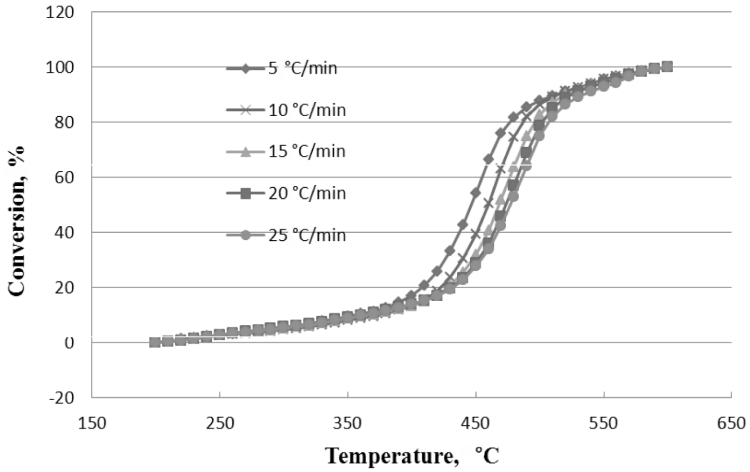

Fig. 2. Conversion vs temperature curves of North-Korean oil shale at different heating rates.

The *dx/dt* vs *T* curves of oil shale obtained through Equations (1) and (2) are shown in Figure 3. It is well known that the reaction region and peak temperatures (T_{max}) are moved to higher temperature with increasing heating rates. The results are in accordance with literature data [14–16].The weight loss process occurs in a shorter time as the heating rate increases. This causes part of the relatively light organic substance, which should volatilize at a lower temperature, to volatilize at a higher temperature, so that the curve moves to a higher temperature region. When reaching a certain temperature, the decrease of conversion can result from the increased thermal lag at higher heating rate.

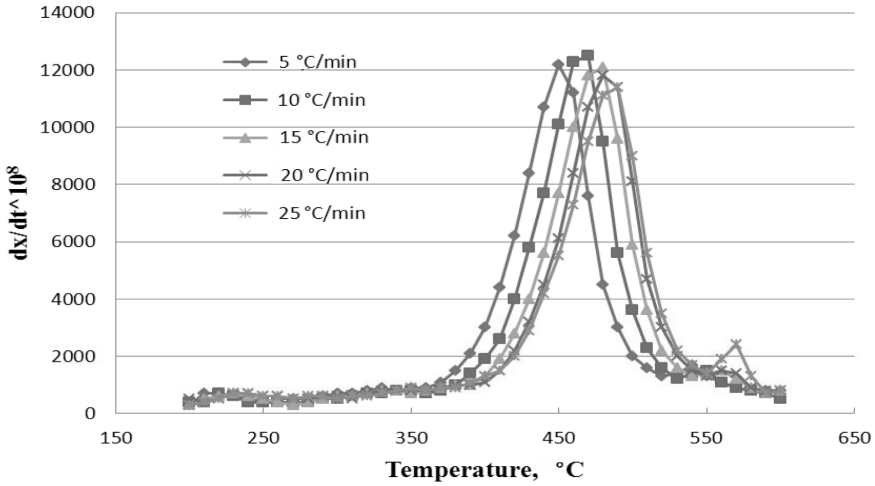

Fig. 3. The *dx*/*dt* vs *T* curves of North-Korean oil shale at different heating rates.

3.1. Friedman procedure

According to Equation (4), 17 values of x ranging from 0.15 to 0.95 at different heating rates are selected. The values of dx/dT and T for each x at different heating rates are determined through the experimental data. According to the slope and intercept of Equation (4), different values of E and A for each x are calculated. The results are presented in Table 2.

From Table 2 it is seen that the apparent activation energy values range from 209 kJ/mol to 359 kJ/mol, corresponding to the fraction conversion x ranging from 15% to 95%. The values of A are in the range of 6.32×10^{12} to 1.99×10^{20}·min^{-1}. The logarithms of A and apparent activation energy E fit the linear kinetic compensation effect (KCE) relation. The KCE regression equation is $\ln A = 0.13E + 1.57$ ($R = 0.9939$), and is discussed in detail elsewhere [17–18]. The results are shown in Figure 4.

Table 2. Results from the Friedman procedure

x, %	E, kJ/mol	A, min^{-1}
15	209.7918078	6.31557×10^{12}
20	210.3729189	9.66675×10^{12}
25	212.010472	6.75613×10^{12}
30	212.3258375	2.52983×10^{12}
35	215.0824331	3.49573×10^{12}
40	216.3854744	2.50634×10^{12}
45	216.8439275	6.87916×10^{12}
50	219.2902898	9.70262×10^{12}
55	220.5018555	1.10503×10^{13}
60	224.2844621	1.8986×10^{13}
65	234.0270495	8.08795×10^{13}
70	243.8195197	3.28186×10^{14}
75	282.3481372	1.10321×10^{17}
80	295.9358492	6.043×10^{17}
85	334.707313	1.02179×10^{20}
90	340.2966246	6.68207×10^{19}
95	359.0040604	1.98872×10^{20}

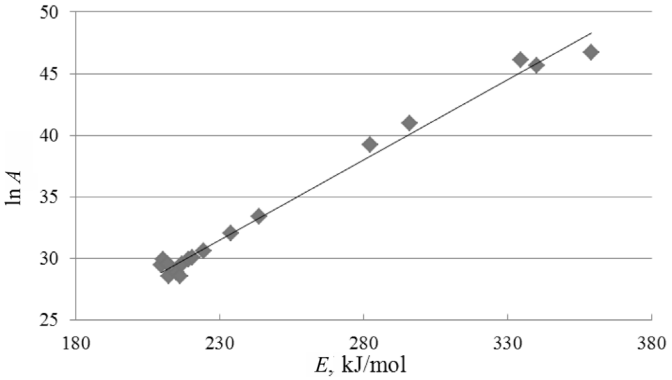

Fig. 4. ln A-E relationship of North-Korean oil shale pyrolysis.

The compensation effect is caused by an increased thermal lag at higher heating rates [19]. The KCE equation reveals a variation of the apparent activation energy with the frequency factor, so both parameters vary with increasing conversion (Figs. 4 and 5). The result is consistent with the literature [17, 19]. In other words, when the procedure is changed, the data (E and A) can be expressed by the KCE relation. This compensation effect can be used to explain the relative magnitudes of E values from analytical methods. It is shown that the same compensation effect affects equally both the Friedman method, and differential and integral methods [17].

It is obvious from Table 2 that the apparent activation energy E increases with increasing conversion x. This is important information concerning the kinetic scheme of fossil fuels [18]. The relationship is depicted in Figure 5. The apparent activation energy E is slightly increasing with increasing conversion. During the increase of conversion, the split of weak chemical bonds results in the production of oil and gas. However, the apparent activation energy E increases dramatically after the value of conversion, during which chemical bonds split, has reached 0.5. Obviously, the pyrolysis process of North-Korean oil shale is an increasing process with increasing apparent activation energy. In contrast, Olivella et al. reported that for Ribesalbes oil shale the dependence of apparent activation energy on conversion degree is of opposite trend [18]. This difference can be attributed to the difference in kerogen type between these two oil shales. So, North-Korean oil shale has kerogen of Type II, whereas the kerogen of Ribesalbes oil shale is of Type I-S [18].

The temperature T_m at the maximum rate of pyrolysis with different heating rates can be derived from dx/dt-T data. From the obtained values of $1/T_m$ and $\ln(\beta/T_m^2)$, the regression slope and intercept in Equation (9) are found and then the apparent activation energy and frequency factor are calculated.

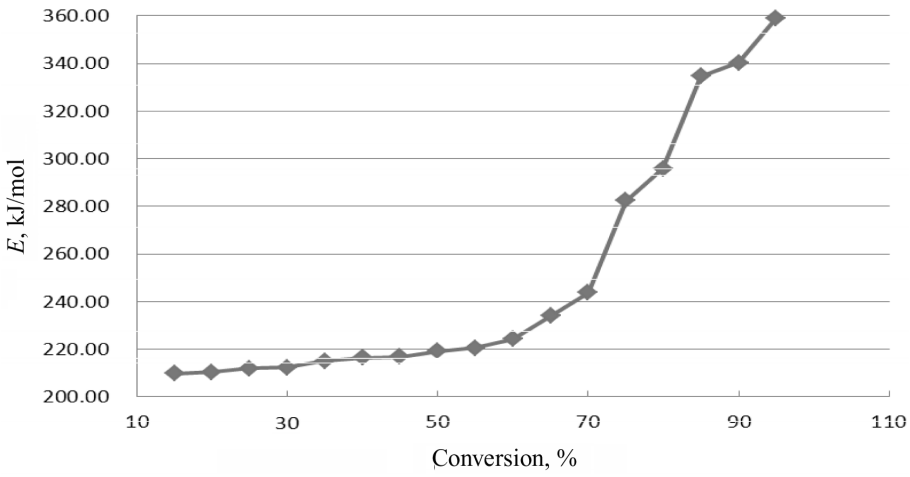

Fig. 5. x-E relationship curve of North-Korean oil shale pyrolysis.

3. 2. Maximum rate method

Table 3 presents the values of T_m, $1/T_m$ and ln (β/T_m^2) at different heating rates obtained using the *dx/dt–T* data. Obviously, the maximum pyrolysis temperature T_m can be achieved by increasing the heating rate. T_m increases from 722.15 to 757.15 K with the increase of the heating rate from 5 to 25 °C/min, respectively. This shift is attributed to that the minimum heat required for the degradation of oil shale is reached later at higher temperatures since the heat transfer is not as effective as it is at lower heating rates [20]. The same phenomena have also been investigated by other researchers. Olivella et al. [17] studied the linear kinetics of pyrolysis of Spanish oil shales and coals. The results showed that there was a shift to higher temperatures during the decomposition of coals and oil shales. Yağmur and Durusoy [14] also found that the temperatures at the maximum pyrolysis rate increased as the heating rate was increased from 10 to 60 K/min. Wang et al. [16] reported the pyrolysis kinetic study of Huadian oil shale, spent oil shale and their mixtures by using thermogravimetric analysis. It was found that T_{max} increased from 453 to 519 °C with increasing heating rate.

The typical plot of ln (β/T_m^2) vs $1/Tm$ depicted in Figure 6 shows that the reaction of oil shale pyrolysis can be described by a first-order reaction

Table 3. Results from the maximum rate method

β, °C/min	T_m, K	$1/T_m$	ln (β/T_m^2)
5	722.15	0.001384754	–11.55502783
10	741.15	0.001349255	–10.91382097
15	746.15	0.00134	–10.521803
20	755.15	0.00132424	–10.25810054
25	757.15	0.001320742	–10.04024694

β is the heating rate, T_m is the temperature corresponding to the maximum pyrolysis rate.

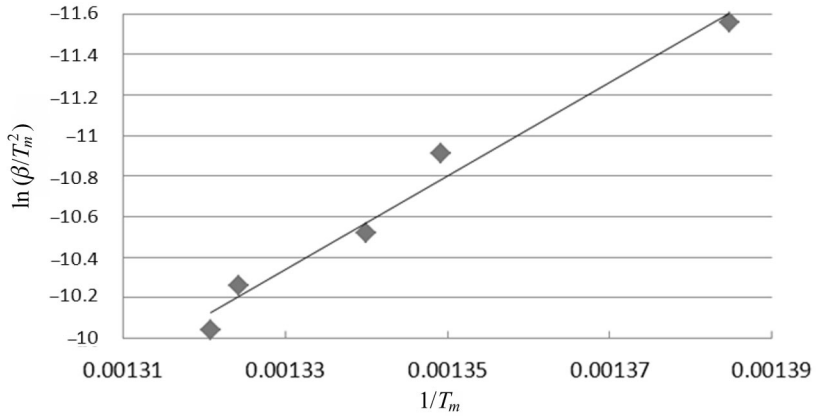

Fig. 6. $1/T_m$ vs ln (β/T_m^2) relationship of North-Korean oil shale pyrolysis.

model in the studied temperature range. From the slope and intercept of the line, the values of E and A can be obtained, being 191.52 kJ/mol and 1.52×10^{13}·min^{-1} (R = 0.9889), respectively. It is found that the values of parameters obtained by the maximum rate method can describe the pyrolysis characteristics at the maximum pyrolysis rate very well.

3.3. Parallel reactions model

It is assumed that the pyrolysis of oil shale can be described using six parallel first-order reactions with different apparent activation energy values (83.68–292.88 kJ/mol). In order to minimize the relative error, the Monte Carlo method is applied to calculating the desired values. The final conversion $x_\infty(j)$ and the apparent frequency factor A_j of each parallel reaction can be obtained from weight loss data. For each parallel reaction, the values of the final conversion $x_\infty(j)$ and the apparent frequency factor A_j are summarized in Table 4.

Table 4 shows that more than 55% of the reactions take place when the apparent activation energy values are in the range of 130–240 kJ/mol during the pyrolysis process. The relative error F of 0.01558 demonstrates a good agreement between the TGA experimental data and calculated results when using the model of six parallel first-order reactions. Therefore it is feasible to describe the pyrolysis process of North-Korean oil shale by the parallel reactions model. The KCE regression equation of ln A_j-E_j is displayed in Figure 7. From the figure, A_j-E_j relationship equations can be written as follows:

$$\ln A_j = 1.998 + 0.1506E_j \, (R = 0.9814) \, . \tag{14}$$

From the above equations of A-E it can be seen that the linear regression coefficient is higher than 0.98. It shows that the apparent activation energy-frequency factor relationship fits the KCE relation. To some degree, the KCE relation based on kinetic parameters provides a clue to recognize whether or not the obtained parameter set (E and A) fits the same mass loss kinetics. If the parameter set (E and A) satisfies the KCE relation, then the kinetics may be correlated with both parameters [22]. Apparent activation energy and frequency factor are two important parameters to investigate the pyrolysis mechanism and the chemical structure of kerogen.

Table 4. Kinetic parameters from the model of six parallel reactions

E_j, kJ·mol^{-1}	E_j, kcal·mol^{-1}	A_j, min^{-1}	$x_\infty(j)$	F
83.68	20	1.5410×10^{7}	0.06434	0.01558
125.52	30	4.5406×10^{8}	0.1327	
167.36	40	3.146×10^{11}	0.3018	
209.20	50	3.264×10^{13}	0.2968	
251.04	60	5.246×10^{17}	0.1529	
292.88	70	3.147×10^{20}	0.05147	

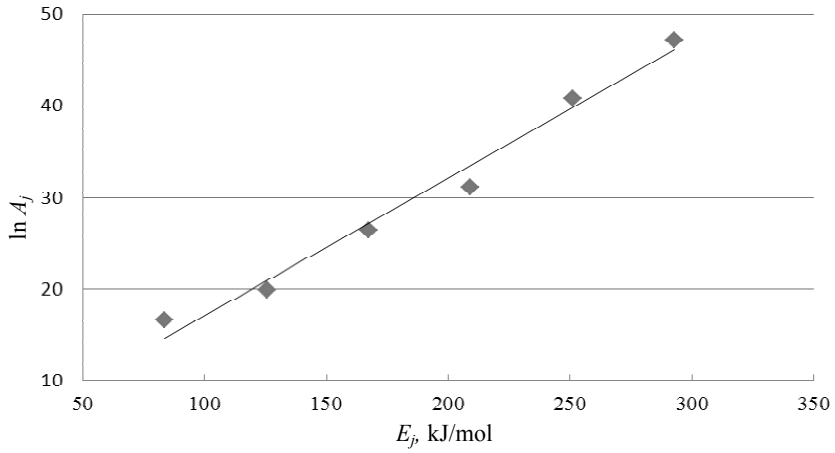

Fig. 7. ln A_j-E_j relationship curve of North-Korean oil shale pyrolysis.

Figure 8 depicts the ln *A*-*E* relationship of North-Korean oil shale pyrolysis in three kinetic models. In the Friedman procedure, it is supposed that the pyrolysis process includes a limited number of continuous reactions, which is indicative of the relationship between kinetic parameters and conversion. The apparent activation energy increases from 209 kJ/mol to 359 kJ/mol when conversion ranges from 0.15 to 0.95. The more intensive the fraction conversion is, the higher is the apparent activation energy. During the heating process, reactions with low apparent activation energy firstly generate water and light hydrocarbon. The reaction can, with increasing temperature, gradually produce shale oil. With increasing temperature, reactions with higher apparent activation energy proceed gradually to afford shale oil.

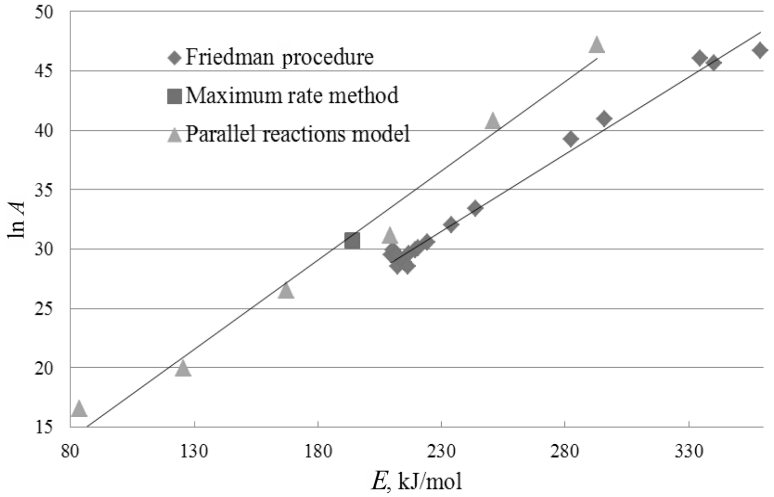

Fig. 8. ln *A*-*E* relationship in three kinetic models of North-Korean oil shale pyrolysis.

The results are in accordance with the earlier literature [23]. The kinetic parameters obtained by the maximum rate method are characteristic of the pyrolysis at maximum pyrolysis rate. The temperature at maximum pyrolysis rate is higher with the increase of heating rate. The parallel reactions model supposes that the pyrolysis process involves N parallel reactions. The parallel reactions with different values of apparent activation energy and frequency factor occur simultaneously. It is found that the values of apparent activation energy are in the range of 80–290 kJ/mol, being mainly between 130 and 240 kJ/mol. The parameters (E and A) of the Friedman procedure and the parallel reactions model obey the KCE relation. The increase of heating rate has two aspects. Firstly, the reaction time is shorter, which favours pyrolysis. Secondly, the difference in temperature inside and outside the oil shale particles is bigger in case of larger particles. Moreover, the pyrolysis gas on the surface of particles may affect the pyrolysis inside the particles because they do not have enough time to diffuse. The pyrolysis of oil shale is influenced by the competition between the two aspects, which may result in the thermal lag. So, the high values of kinetic parameters (E and A) and the related compensation effect result from the thermal lag. It is shown that in the Friedman procedure and the parallel reactions model there is a kinetic compensation effect (KCE) between various constants.

The apparent activation energy value calculated from the proposed kinetic model is similar to that of Spanish oil shale but higher than those of other oil shales reported in the literature (Table 5). However, the subject studies were not carried out under similar conditions.

The pyrolysis process of oil shale as a kind of polymer with a three-dimensional structure may involve the rupture of different types of chemical bonds with different values of energies [20]. The chemical bonds with low activation energy, such as C–O bond, C–S bond, are broken in the beginning of the pyrolysis process, resulting in H_2O, CO_2 and H_2S and other light hydrocarbon products. With increasing temperature, chemical bonds with medium activation energy begin to split, for example, the side chains at β-site of aromatics and alicyclic hydrocarbon. Shale oil is mainly generated in this process. The split of chemical bonds with high apparent activation energy mainly happens in aromatic rings, heterocyclic compounds and alicyclic compounds at a higher temperature. H_2, CH_4, NH_3, CO and coke are released at the end of the process.

Table 5. Comparison of apparent activation energy values and the reaction order determined in the study with literature data

Reference	Process	Oil shale	E, kJ·mol^{-1}	n
Present study	Pyrolysis	North Korean	193.87	1
[14]		Göynük, Turkey	2.2	1
[16]		Chinese	64	1
[17]		Spanish	195	1
[21]		Turkish	111.6	1
[19]	Combustion	Göynük, Turkey	6.9	1

4. Conclusions

According to the Friedman procedure, the more intensive the fraction conversion is, the higher is the apparent activation energy. The apparent activation energy values range from 209 kJ/mol to 359 kJ/mol, corresponding to the fraction conversion x ranging from 15% to 95%. The maximum rate method shows that the apparent activation energy and the frequency factor are 191.52 kJ/mol and 1.51×10^{13} min^{-1}, respectively, when the maximum pyrolysis rate is in the 722.15–757.15 K temperature range. Compared to the maximum rate method, the Friedman procedure provides a better fit of data for North-Korean oil shale pyrolysis. By the parallel reactions model it is demonstrated that the values of apparent activation energy are in the range of 80–290 kJ/mol, being mainly between 130 and 240 kJ/mol. The kinetic models provide more reliable parameters for characterising the oil shale retorting process and identifying the chemical structure of oil shale kerogen. The parallel reactions model is more suitable than the Friedman procedure to describe the process due to the complicated pyrolysis process of oil shale. In the Friedman and parallel reactions methods the kinetic compensation effect (KCE) is kept between various constants.

The pyrolysis reactions with low activation energy result mainly from the breaking of weak chemical bonds such as C–O and C–S bonds. Pyrolysis reactions with high activation energy may be involved in the breaking up of the C–C bond, dehydrogenation, and condensation of polycyclic aromatics.

Nomenclature

A, A_j	frequency factor, s^{-1};
E, E_j	apparent activation energy, kJ/mol;
k	reaction rate constant, s^{-1};
R	general gas constant, 8.314 kJ/mol·K;
t	pyrolysis time, s;
T	pyrolysis temperature, °C;
x, x_j	fractional conversion of oil shale;
$\beta = dx/dT$	constant heating rate, °C/s;
$h = T_{j+1} - T_j$	temperature interval;
j	point numbers of numerical derivatives;
T_m	temperature at the maximum reaction rate;
N	number of parallel reactions;
$x_\infty(j)$	total fractional conversion;
F	relative error;
M	number of experimental data sets.

Acknowledgements

The authors are grateful for the financial support from the National Basic Research Program of China (973 programs, No. 2014CB744302), the Taishan Scholar Constructive Engineering Foundation of Shandong province, China (No.ts20120518) and the Science Foundation of China University of Petroleum, Beijing, China (No. KYJJ2012-06-32).

REFERENCES

1. Sert, M., Ballice, L., Yüksel, M., Sağlam, M. The effects of acid treatment on the pyrolysis of Göynük oil shale (Turkey) by thermogravimetric analysis. *Oil Shale*, 2012, **29**(1), 51–62.
2. Qian, J. L., Wang, J. Q., Li, S. Y. Oil shale development in China. *Oil Shale*, 2003, **20**(3S), 356–359.
3. Yanik, J., Seçim, P., Karakaya, S., Tiikma, L., Luik, H., Krasulina, J., Raik, P., Palu, V. Low-temperature pyrolysis and co-pyrolysis of Göynük oil shale and terebinth berries (Turkey) in an autoclave. *Oil Shale*, 2011, **28**(4), 469–486.
4. Kök, M. V. Geological considerations for the economic evaluation of Turkish oil shale deposits and their combustion-pyrolysis behavior. *Energ. Source. Part A*, 2010, **32**(4), 323–335.
5. Williams, P. T, Ahmad, N. Investigation of oil-shale pyrolysis processing conditions using thermogravimetric analysis. *App. Energ.*, 2000, **66**(2), 113–133.
6. Li, S. Y., Yue, C. T. Study of pyrolysis kinetics of oil shale. Fuel, 2003, **82**(3), 337–342.
7. Dogan, O. M, Uysal, B. Z. Non-isothermal pyrolysis kinetics of three Turkish oil shales. Fuel, 1996, **75**(12), 1424–1428.
8. Torrente, M. C., Galan, M. A. Kinetics of the thermal decomposition of oil shale from Puertollano (Spain). Fuel, 2001, **80**(3), 327–334.
9. Tiwari, P., Deo, M. Compositional and kinetic analysis of oil shale pyrolysis using TGA-MS. Fuel, 2012, **94**, 333–341.
10. Williams, P. T., Ahmad, N. Influence of process conditions on the pyrolysis Pakistani oil shales. Fuel, 1999, **78**(6), 653–662.
11. Aboulkas, A, El Harfi, K. Study of the kinetics and mechanisms of thermal decomposition of Moroccan Tarfaya oil shale and its kerogen. *Oil Shale*, 2008, **25**(4), 426–443.
12. Abu-Qudais, M., Jaber, J. O., Sawalha, S. Kinetics of pyrolysis of Attarat oil shale by thermogravimetry. *Oil Shale*, 2005, **22**(1), 51–63.
13. Luo, B. J., Wang, C. J., Dong, C. M., Lin, J. H. Organic geochemical characteristics of oils from Anzhou basin, DPR Korea. *Acta Petrolei Sinica*, 1995, **16**(4), 40–47 (in Chinese).
14. Yağmur, S., Durusoy, T. Kinetics of the pyrolysis and combustion of Göynük oil shale. *J. Therm. Anal. Calorim*., 2006, **86**(2), 479–482.
15. Meng M., Hu, H. Q., Zhang, Q. M., Li, X., Wu, B. Pyrolysis behaviors of Tumuji oil sand by thermogravimetry (TG) and in a fixed bed reactor. *Energ. Fuel*., 2007, **21**(4), 2245–2249.

16. Wang, Z. J., Deng, S. H., Gu, Q., Zhang, Y. M., Cui, X. J., Wang, H. Y. Pyrolysis kinetic study of Huadian oil shale, spent oil shale and their mixtures by thermo-gravimetric analysis. Fuel Process. Technol., 2013, **110**, 103–108.
17. Olivella, M. A., De Las Heras, F. X. C. Evaluation of linear kinetic methods from pyrolysis data of Spanish oil shales and coals. *Oil Shale*, 2008, **25**(2), 227–245.
18. Olivella, M. A., De Las Heras, F. X. C. Nonisothermal thermogravimetry of Spanish fossil fuels. *Oil Shale*, 2006, **23**(4), 340–355.
19. Narayan, R., Antal, M. J. Thermal lag, fusion and the compensation effect during biomass pyrolysis. *Ind. Eng. Chem. Res*., 1996, **35**(5), 1711–1721.
20. Yağmur, S., Durusoy, T. Oil shale combustion kinetics from single thermo-gravimetric curve. *Energ. Source. Part A*, 2009, **31**(14), 1227–1235.
21. Li, S. Y., Yue, C. T. Study of different kinetic models for oil shale pyrolysis. *Fuel Process. Technol*., 2004, **85**(1), 51–61.
22. Liu, N. A., Wang, B. H., Fan, W. C. Kinetic compensation effect in biomass thermal decomposition. *Fire Safety Science*, 2002, **11**(2), 63–70 (in Chinese).
23. Kok, M. Geological considerations for the economic evaluation of Turkish oil shale deposits and their combustion-pyrolysis behavior. *Energ. Source. Part A*, 2009. **32**(4), 323–335.

Received October 30, 2013